doi: 10.17116/engoftalma20151316-2

Abnormal distribution of trace elements in keratoconic corneas

S.E. AVETISOV, V.R. MAMIKONYAN, I.A. NOVIKOV, L.S. PATEYUK, G.A. OSIPYAN, N.P. KIRYUSHCHENKOVA

Research Institute of Eye Diseases, 11 A, B, Rossolimo St., Moscow, Russian Federation, 119021

Our understanding of etiology and pathogenesis of many disorders, corneal included, greatly relies on existing knowledge in human biochemistry and biophysics. This study was **aimed** at chemical mapping of normal and keratoconic corneas. **Material and methods.** Modern methods of analytical chemistry, such as X-ray fluorescence and energy-dispersive X-ray spectroscopy on the basis of scanning electron microscopy, were adapted to the needs of cornea research. Normal human corneas obtained postmortem and corneal buttons obtained during penetrating keratoplasty were analyzed. **Results.** In keratoconus, abnormal accumulation of iron, copper, and zinc was found in the periphery of the buttons, i.e. in the zone of visible pigmentation (Fleischer ring), while the center — the ectatic zone — demonstrated a total deficiency of trace elements. This data suggests that keratoconus pathogenesis is associated with impaired mineral metabolism and formation of a physicochemical barrier in corneal tissues with subsequent keratectasia. The authors discuss several possible vicious circles involved.

Keywords: *keratoconus, Fleischer ring, pathogenesis, cornea, elemental analysis, XRF, SEM-EDS.*

Vestnik_Oftalmologii_2015-6_34EN

Keratoconus (KC) is a non-inflammatory degenerative disorder of the cornea associated with its conical transformation and progressive central thinning. There is no scientific consensus on etiology and pathogenesis of the disease: despite the vast amount of research and multiple theories and hypotheses, ultrastructural mechanisms underlying this particular type of corneal protrusion remain unclear.

Eye examination in KC reveals specific morphological changes and clinical signs, such as annular pigmentation (Fleischer ring) at the base of the cone [1], i.e. within the paracentral zone of the cornea [2]. According to published data, the ring is the most common slit-lamp sign of KC [1, 3] and since it is usually found in moderate and advance cases — also a sign of disease progression [4]. It is believed to result from hemosiderin deposition in basal epithelial cells due to distorted corneal sphericity and associated tear film disorder [1].

The presence of hemosiderin was established long ago by qualitative reaction on iron [5]. After modern methods of analytical chemistry became available, other elements have been also identified [6] but have never been studied in terms of spatial distribution.

From all methods suitable for determination of elemental composition of biological objects, X-ray spectral analysis is the most widely used. It consists of identification of X-ray emission from the sample under certain excitation.

The latter can be achieved with either X-rays — the method is then called X-ray fluorescence (XRF) spectrometry, — or electron beams — then we are taking about energy-dispersive X-ray spectroscopy on the basis of scanning electron microscopy (SEM-EDS).

In this study, modern methods of analytical chemistry were adapted to enable qualitative and semi-quantitative analysis of element distributions in normal and KC corneas.

We aimed to analyze trace elements content and distribution in different zones (central vs. paracentral) and layers of normal and keratoconic corneas.

Material and methods

Despite XRF and SEM-EDS both being good at elemental analysis and capable of high resolution, each possesses certain advantages and disadvantages. For example, XRF is characterized by greater detection sensitivity and lower threshold of detectability, while SEM-EDS has greater spatial resolution and higher degree of the localization accuracy.

XRF

In order to study elemental composition of normal and keratoconic corneas, 7 healthy corneal buttons from male cadaveric donors aged 25-35 and 5 corneal buttons from 3 male and 2 female patients aged 27-31 who underwent penetrating keratoplasty (PKP) for KC stage III [7] were obtained.

Semi-quantitative elemental analysis of corneal buttons was performed with a ReSPEKT XRF analyzer (TOLOKONNIKOV, Russia) under the following conditions: accelerating voltage of 30 kV, exposure of 300 sec, copper cathode.

Corneal buttons were cut off with 7-8 mm trephines.

For correspondence:
Pateyuk Lyudmila Sergeevna — postgraduate
e-mail: sweethailtoyou@mail.ru

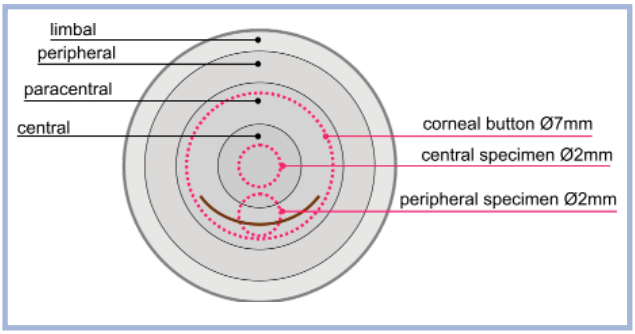

Fig. 1. **Cornea sampling for XRF.**

Optical zones of the cornea [2] are marked out: central – a circle of 4 mm diameter; paracentral – a 2 mm wide ring with the outer diameter of 8 mm; peripheral – a 1.5 mm wide ring with the outer diameter of 11 mm; limbal – an up to 0.5 mm wide ring with the outer diameter of 12 mm. Borders a Ø 7 mm corneal button and Ø 2 mm corneal specimens (central and peripheral) are shown with red dotted lines. A brownish arch-shaped line in the inferior segment of the cornea represents the Fleischer ring.

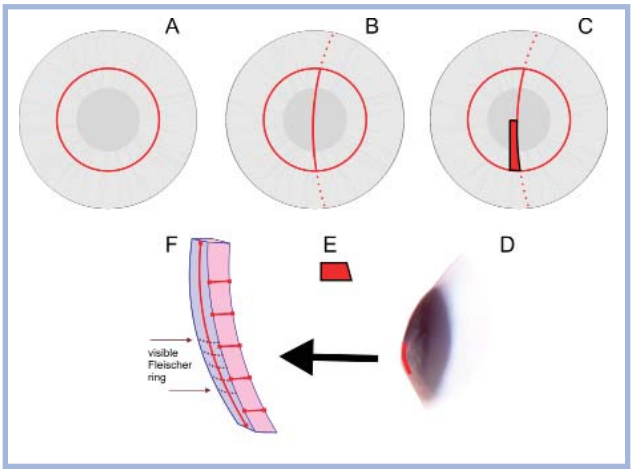

Fig. 2. **Cornea sampling for SEM–EDS.**

Solid red lines in A-C represent the borders of a Ø 7 mm corneal button and a sagittal oblique cut through its center. Location and orientation of the specimen to be removed are shown in C (front view) and D (side view). Trapezoidal cross-section of the specimen is illustrated in E. A total of 6 scan lines were preselected: 1 line ran across the anterior face of the prism-shaped specimen along its long edge and 5 subparallel anterior-posterior lines ran across its beveled face (F). The Fleischer ring zone within the specimen is indicated by brownish arrows (F).

In order to separately analyze central and paracentral zones of the cornea, which in case of KC correspond to the ectatic and Fleischer ring zones, respectively, two specimens (central and peripheral) were obtained from all the buttons with a 2 mm trephine (**Fig. 1**). These specimens were then evaporated in a dust-free chamber under standard conditions of 65% RH, +20°C, and atmospheric pressure.

SEM-EDS

This part aimed at studying elemental composition of normal and keratoconic corneas in 6 healthy corneal buttons obtained from male cadaveric donors aged 25-35 and 5 corneal buttons obtained from 4 male and 1 female patients aged 28-34 who underwent penetrating keratoplasty (PKP) for KC stage III.

For semi-quantitative elemental analysis of corneal buttons an EVO LS 10 scanning electron microscope (Carl Zeiss Group, Germany) supplemented with an Oxford X-Max 50 EDS-analyzer (Oxford Instruments, United Kingdom) was used. Back-scattered electron (BSE) images thus obtained enabled micro-mapping of trace elements.

Corneal buttons were cut off with 7-8 mm trephines.

Once removed, the buttons were quick-frozen with liquid nitrogen (in order to prevent migration of trace elements in corneal tissues) and lyophilized at the pressure of 50 Pa and the temperature of –5°C. Then a sagittal oblique cut was made through the center of each button and from there full-thickness specimens (4 mm long and 0.6 mm wide) were excised, shaped in the form of a trapezoidal rectangular prism (**Fig. 2**). In order to reveal elemental composition of the cornea at different distances from its center and at different depths from its anterior surface, 6 scan lines were preselected for each of the prism-shaped specimens: 1 line (1000 scan positions) ran across the anterior face of the prism along its long edge and 5 subparallel anterior-posterior lines (850 scan positions each) ran across its beveled face. X-ray emission was recorded within a wide range of energies — from 4.445 to 9.982 keV, which is sufficient to test biological samples and to achieve the purpose of current research. Scanning conditions were set as follows: extended pressure mode (EP), accelerating voltage of 20 kV, current at the sample of 520 pA, exposure of 18 sec.

To prevent the sample from burning up, we ensured a 4-μm drift of the electron beam. Obtaining a whole line profile took from 7.5 to 19 hours, detector dead time included.

Standard methods of spectral X-ray data processing, based on reconstruction of a linear baseline under each of the emission peaks, are associated with significant inaccuracy (which is the greater, the smaller the peak is) in case of relatively low concentrations of trace elements in biological objects (cornea in particular).

To solve this problem, we developed an original method of baseline correction, which implies the use of Kα lines of titanium (Ti), vanadium (V), cobalt (Co), gallium (Ga), and germanium (Ge) as key points for interpolation similar to that of Bézier. The reason for these particular elements to be chosen is that they are extremely rare and, thus, can be considered absent in the body. If present, however, they still do not participate in metabolism. Taking this into account, we can claim that these elements do not contribute to X-ray emission and that intensities in corresponding points are baseline. That makes us able to calculate true emission intensities for any of the elements between V and Co, as well as Co and Ga, by subtracting interpolated values from the number of impulses registered by the detector (**Fig. 3**).

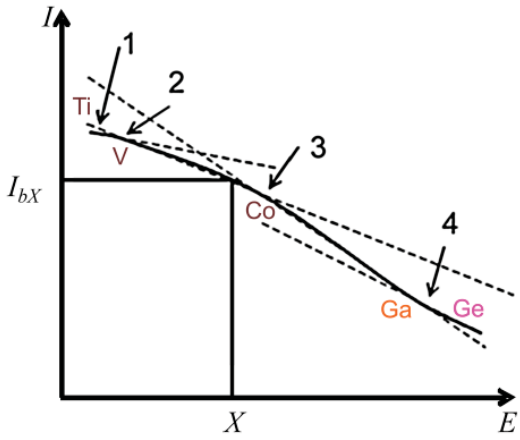

$$k_{12} = (I_2 - I_1)/(E_2 - E_1) \qquad t = (E_x - E_2)/(E_3 - E_2)$$
$$k_{23} = (I_3 - I_2)/(E_3 - E_2) \qquad w_2 = (\cos(\pi t) + 1)/2$$
$$k_{34} = (I_4 - I_3)/(E_4 - E_3) \qquad w_{23} = (\cos(\pi(2t - 1)) + 1)/2$$
$$k_2 = (k_{12} + k_{23})/2 \qquad w_3 = 1 - w_2$$
$$k_3 = (k_{23} + k_{34})/2 \qquad w_S = w_2 + w_{23} + w_3$$

$$I_{bX2} = I_2 + k_2(E_x - E_2) \qquad W_2 = w_2 / w_S$$
$$I_{bX23} = I_2 + k_{23}(E_x - E_2) \qquad W_{23} = w_{23} / w_S$$
$$I_{bX3} = I_3 + k_3(E_x - E_3) \qquad W_3 = w_3 / w_S$$

$$I_{bX} = I_{bX\,2}W_2 + I_{bX\,23}W_{23} + I_{bX\,3}W_3$$

Fig. 3. **Baseline correction formula and its graphical explanation.**

Absolute determination of element content in this approach is complicated, but it plays no role in achieving our ends. What is important is that the method allows clear description of chromium (Cr), manganese (Mn), iron (Fe), nickel (Ni), copper (Cu), and zinc (Zn) concentration variability in 'light' matrices.

All line profiles data were processed as described above.

To reduce the effect of random errors associated with structural irregularity of the tissue, all points were binned into the groups of 40.

Visualization was done with Surfer 8.0 mapping software (Golden Software, Inc., USA), which is capable of interpolating irregularly spaced data into a regularly spaced grid in order to produce different types of maps.

Results

It has been found that keratoconus is associated with abnormal accumulation of iron, copper, and zinc in the periphery of the buttons, i.e. in the zone of visible pigmentation (Fleischer ring), while the center — the ectatic zone — demonstrated a total deficiency of trace elements.

XRF

Both central and peripheral specimens from normal corneal buttons demonstrated similar concentrations of Fe, Cu, and Zn, whereas in keratoconic corneas there was an evident accumulation of all three elements in the periphery of the buttons and a complete deficiency of these in the ectatic area (**Table 1**). Copper content in peripheral specimens from keratoconic buttons was significantly higher (20.6 times) than that in any of the healthy corneal specimens; the same for Zn and Fe — 7.8 and 3.7 times, respectively. Microconcentrations of lead and nickel were also present in the midperiphery of keratoconic corneas. As for calcium, it was absent in healthy corneas, but present in similar concentration in both central and peripheral specimens from keratoconic corneas.

SEM-EDS

After having obtained BSE images and binned data from 5 transverse line profiles (**Fig. 4**), we applied the Surfer software to perform interpolation to produce micromaps of Fe, Cu, and Zn concentration variability in different layers of the cornea (**Fig. 5**).

Iron, copper, and zinc were found to be rather evenly distributed within a normal corneal button. Iron, how-

Table 1. **XRF data on metal content and distribution in normal and keratoconic corneas**

Metal	Corneal buttons with no signs of impairment (center and periphery)	Corneal buttons obtained during penetrating keratoplasty for KC III	
		center	periphery
Fe	+ (equal concentrations)	—	3.7 times as high as that in normal cornea
Cu	+ (equal concentrations)	—	20.6 times as high as that in normal cornea
Zn	+ (equal concentrations)	—	7.8 times as high as that in normal cornea
Pb	—	—	+
Ni	—	—	+
Ca	—	+ (center equals periphery)	

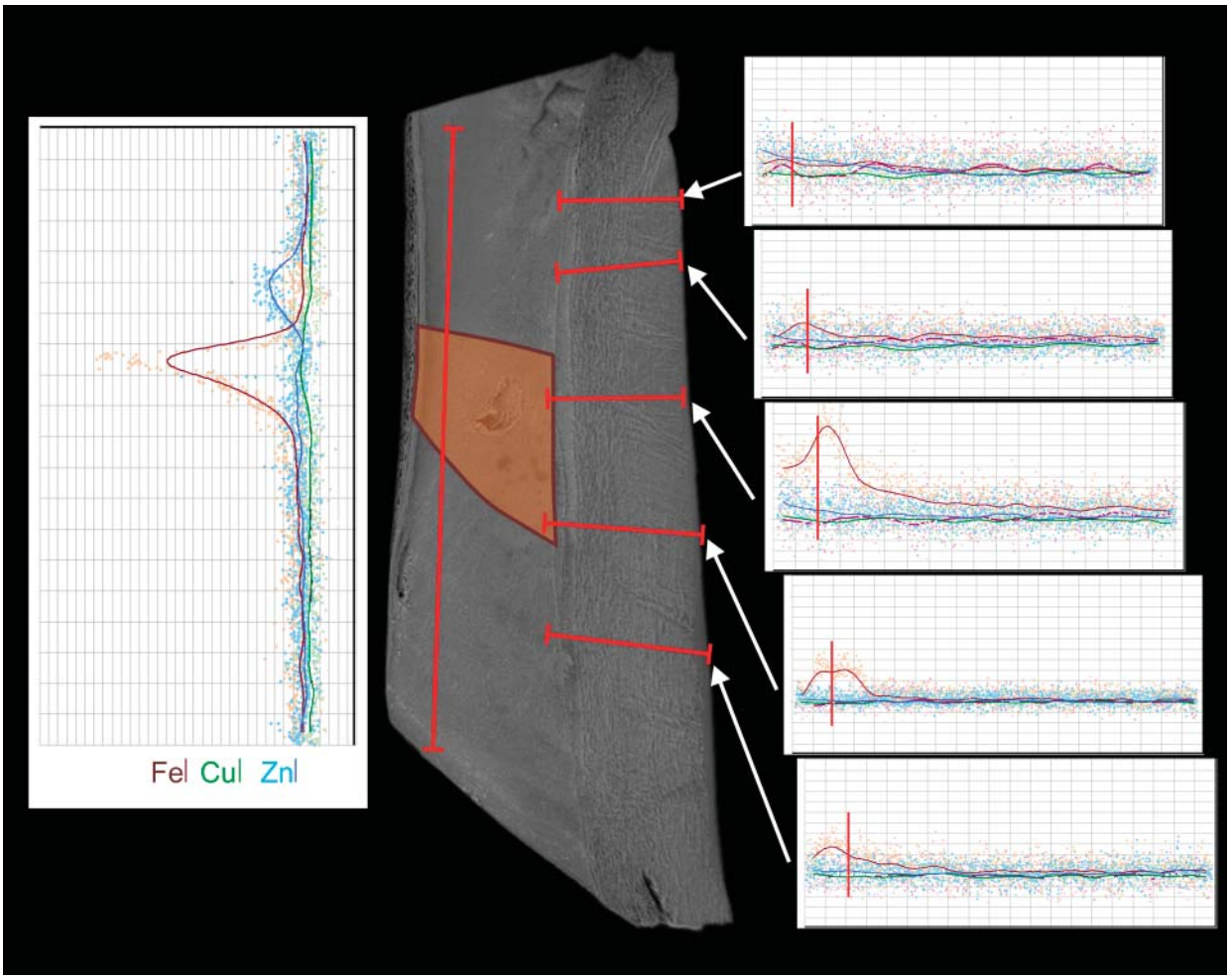

Fig. 4. **BSE image of one of the corneal specimens and chemical analysis data (SEM-EDS).**

This a BSE image of a full-thickness trapezoidal rectangular prism-shaped specimen, whose beveled face is a sagittal oblique cut through the center of a Ø 7 mm corneal button. EDS scan lines are shown in red. Corresponding line profiles are provided. Bowman's membrane position is marked by purple vertical lines. The Fleischer ring zone is shown in brownish.

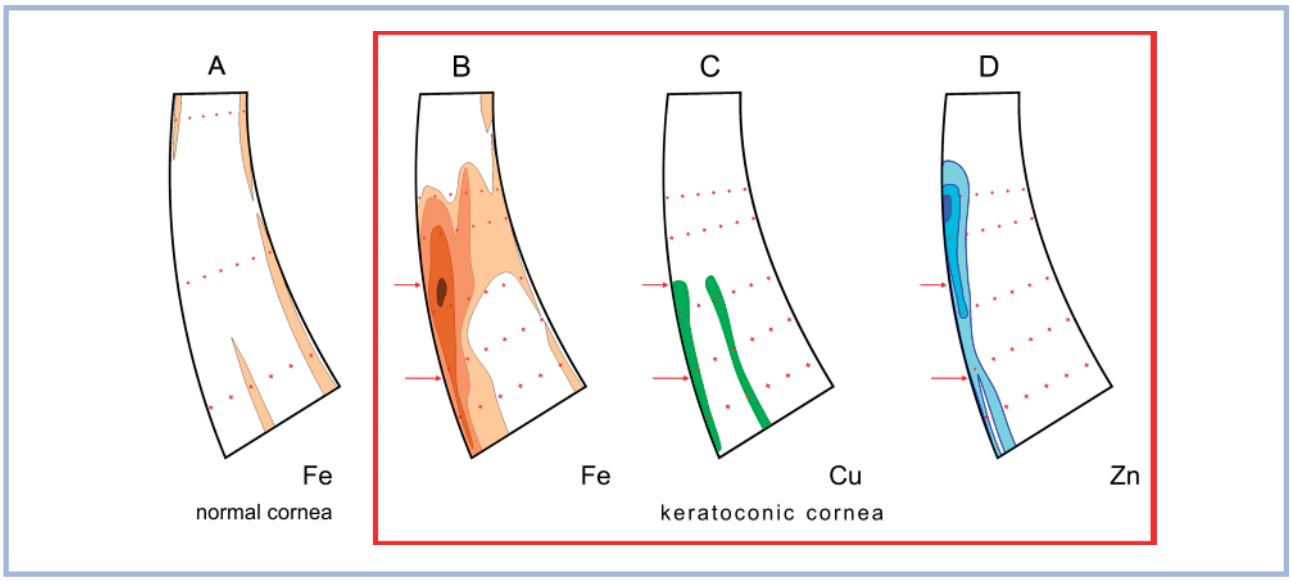

Fig. 5. **Interpolation–based fields of trace elements distribution according to SEM–EDS.**

A — Iron distribution in healthy corneal buttons; B — Iron distribution in keratoconic corneal buttons; C — Copper distribution in keratoconic corneal buttons; D — Zinc distribution in keratoconic corneal buttons. The Fleischer ring zone is indicated by red arrows.

Table 2. **The role of metal-dependent enzymes in connective tissues metabolism**

Metal	Effect on enzyme activity	Role of enzymes	Enzyme deficiency outcomes
Fe	Cofactor for prolyl hydroxylase and lysyl hydroxylase	Post-translational modification of the pre-pro-peptide	Diminished or abnormal collagen synthesis
Cu	Cofactor for lysyl oxidase	Covalent bonding between tropocollagen molecules	Diminished or abnormal collagen synthesis
Zn	Cofactor for connective tissue collagenase and matrix metalloproteinases	Breakdown of proteins	Impaired breakdown of collagen
Fe, Cu	Inhibitor of hyaluronidases	Decrease of glycosaminoglycans viscosity in the extracellular matrix	Increase of glycosaminoglycans viscosity, which leads to abnormal extracellular matrix biomechanics and transport
Cu, Zn	Cofactor for superoxide dismutases	Dismutation of superoxide O_2^- into oxygen O2 and hydrogen peroxide H_2O_2	Oxidative stress in tissues

ever, was mainly concentrated at the periphery and in posterior corneal layers (**see Fig. 5, a**).

In keratoconus, an abnormal accumulation of iron was observed in anterior and midperipheral cornea, i.e. within the Fleischer ring zone (**see Fig. 5, b**). Analogous redistribution was shown for copper and zinc (**see Fig. 5, c and d**).

Calcium was found in similar concentrations in both the center and midperiphery of keratoconic corneas.

SEM-EDS also revealed the presence of magnesium in all of the buttons. Qualitative analysis showed that KC was associated with Mg content two times higher than normal in both central and midperipheral cornea.

According to a number of authors, these are pathological changes in extracellular matrix of corneal stroma that underlie the development of KC: corneal collagen fibers are known to decrease in number and become disordered [8-10].

Due to direct participation of many trace elements (especially metals) in enzyme activity, their presence, concentration, and bioavailability are the factors that determine collagen and elastin fibers synthesis and breakdown [11-15].

Collagen anabolism is regulated by hydroxylases, lysyl oxidase, and glycosyltransferases. Prolyl hydroxylase as well as lysyl hydroxylase is responsible for post-translational modification of collagen pre-pro-peptide and contains an iron ion in its active site. Lysyl oxidase, a copper-carrying enzyme, mediates collagen cross-linking. In the presence of magnesium (the cofactor) glycosyltransferases perform glycosylation of hydroxylysine in collagen fibers [12-15] (**Table 2**).

Collagen catabolism is regulated by metal-dependent enzymes: metalloproteinases and collagenases. Matrix metalloproteinases are the family of extracellular Zn-dependent endopeptidases that promote degradation of all kinds of extracellular matrix proteins, including collagen. Connective tissue collagenase is also a Zn-carrying enzyme, involved in peptide bonds cleavage (**see Table 2**) [12-15].

Not only collagen fibrils but also the ground substance (physicochemical state of glycosaminoglycans in particular) is in charge of extracellular biomechanics and transport in connective tissues. Glycosaminoglycans viscosity increases in the presence of iron or copper ions due to inhibition of hyaluronidase activity (**see Table 2**) [12-15].

Since cornea is known to receive oxygen directly from the air and to have high oxygen permeability [16-20], corneal cells, fibrils, and ground substance are as abundantly exposed to free oxygen as nothing else in the human body. Thus, a strong antioxidant defense is required. Superoxide dismutases (SODs) are the enzymes that protect tissues from oxidative stress. In humans they are cofactored by either copper and zinc (the major functional and an important structural component correspondingly), or manganese. SOD1 is predominantly found in the cytoplasm, SOD2 — in the mitochondria, SOD3 — in the extracellular matrix (**see Table 2**) [21].

In some pathological conditions mineral metabolism in the eye can become disturbed. Special attention has been always paid to iron [22, 23]. Corneal pigment deposition is not uncommon. Hudson-Stahli line is often found in elderly patients [24,25]. Stocker's line is typical of corneas with pterygium [26]. Orthokeratology lens wearers may develop a pigmented arc or line, which is believed to result from corneal reshaping [27, 28]. Intrastromal corneal ring segments implantation is associated with appearance of annular pigmentation [29]. Iron lines can be seen after refractive corneal surgery, such as radial keratotomy [30], photorefractive keratectomy [31], and laser-assisted in situ keratomileusis [32]. Ferry's line is associated with filtering blebs [33]. Scleral mineral metabolism was also proved impaired in myopia [34].

Taking into consideration the phenomenal participation of metal ions in normal functioning of extracellular matrix on the one hand and revealed impairment of mineral metabolism in keratoconic corneas on the other, an assumption can be made that metabolic changes are not just a consequence but a pathogenetic mechanism of KC.

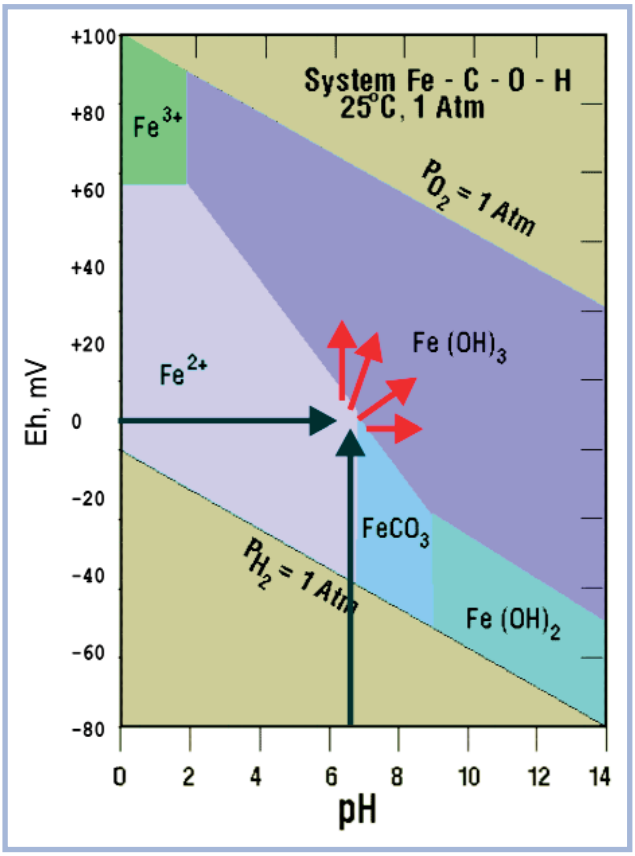

Fig. 6. **Pourbaix diagram of iron.**

Black arrows indicate the physicochemical balance of healthy cornea, in which Fe is bioavailable and forms water-soluble compounds. Red arrows represent the shift in Eh and pH values that takes place in keratoconic corneas and results in formation of water-insoluble bio-unavailable iron compounds.

Disorganization of stromal extracellular matrix may affect metal ion transport leading to mineral deposition in tissues. The absence of minerals within the ectatic area can in turn result in abnormal functioning of metal-dependent enzymes, subsequent suppression of collagen synthesis and disorganization of the extracellular matrix. Thus, the pigmented ring at the base of the cone, considered as just a symptom, may be the actual cause of keratectasia.

According to Goldschmidt's geochemical classification, Cu, Zn, Fe, Pb, and Ni are transitional metals of the 4th period and constitute a group of chalcophile elements. These elements share common physicochemical properties that can be presented in the form of Pourbaix diagrams (also known as Eh-pH or pE/pH diagrams). These diagrams map out possible stable phases of aqueous electrochemical systems having pH (acidity/basicity) and Eh (oxidation/reduction potential) values as the horizontal and vertical axes, correspondingly (**Fig. 6**).

For instance, when Eh of an aqueous solution is about 0 mV, which is typical of the cornea [35], and pH is neutral, which is typical of all living systems, including the human body, atoms of iron are water-soluble and bio-

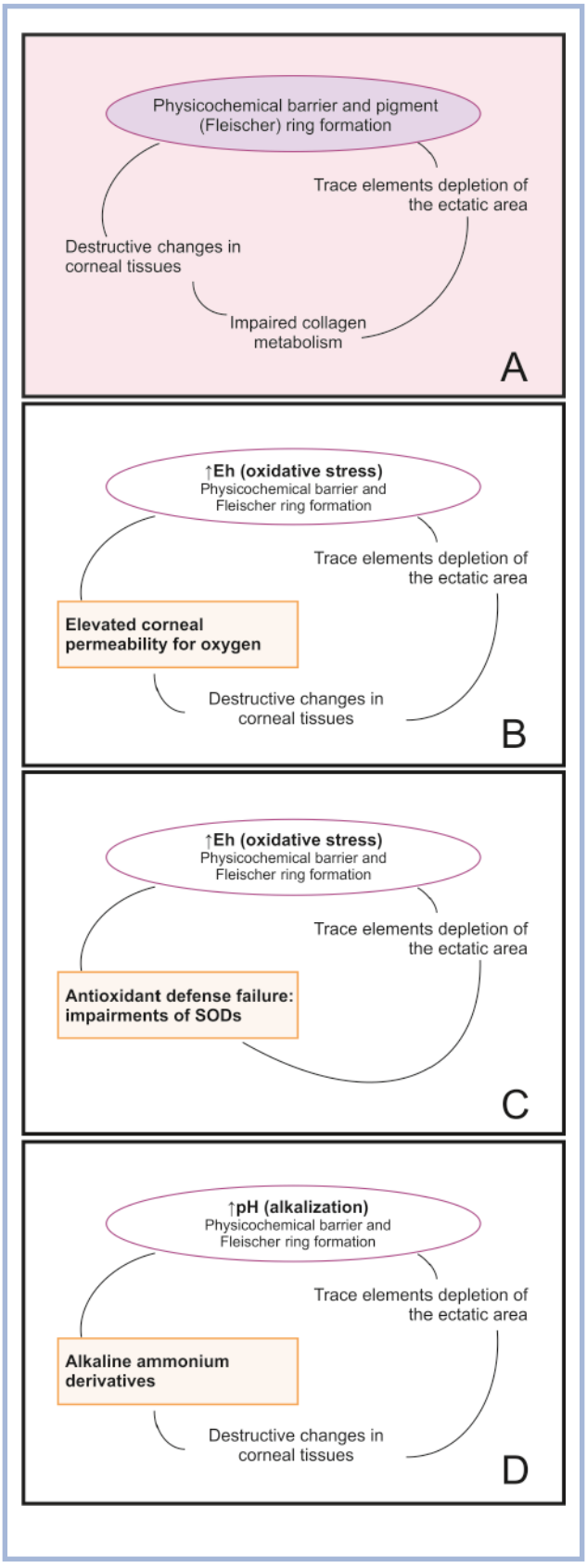

Fig. 7. **Cause and effect relationships in keratoconic cornea.**

A — a principle scheme of cause and effect relationships in keratoconus; B — chain of causation in case of increased oxygen permeability of corneal epithelium; C — chain of causation in case of superoxide dismutase dysfunction; D — chain of causation in case of a shift of corneal pH.

available. An increase of Eh and/or pH values results in formation of water-insoluble precipitates in the tissues. The same applies to zinc, copper, lead, and nickel.

Thus, precipitation of chalcophile elements in corneal tissues followed by pigmented ring (Fleischer ring) development results from a pH and/or Eh shift. The latter in turn is due to a certain physicochemical barrier at the boundary of the ectasia. Characteristic patterns of line profiles provide us with evidence that supports the existence of such a barrier. On the assumption that the mentioned barrier is both the cause and effect of degenerative and/or dystrophic processes in keratoconic corneas, several vicious circles can be suggested **(Fig. 7, a)**.

Reduction potential measures the tendency of chemical species to acquire electrons and can be increased by excessive amounts of oxygen; therefore, anomalous oxygen permeability of the cornea is a possible contributor to an Eh increase. Since corneal permeability is predominantly regulated by its epithelium, epithelial dysfunction should be regarded as a possible cause for physicochemical barrier formation, which manifests itself as the Fleischer ring and leads to trace elements depletion and ectatic transformation of the central cornea. At the same time epithelial dysfunction with subsequent physicochemical barrier formation can be caused/aggravated by destructive changes in diseased corneal tissues **(see Fig. 7, b)**.

A failure of antioxidant defense (dysfunction of SODs) in case of trace elements deficiency is another possible reason for Eh increase as it provokes oxidative stress in corneal tissues **(see Fig. 7, c)**.

Changes in corneal pH can be caused by some external factors, like tear acidity. High pH possibly disturbs ion equilibrium and starts the process of pigmented ring development and subsequent corneal degeneration [6]. Again, a pH rise can itself be a subsequence of destructive processes in keratoconic corneas associated with a breakdown of essential proteins and formation of alkaline ammonium derivatives **(see Fig. 7, d)**.

Conclusion

The distribution pattern of trace elements in keratoconic corneas supports the presence of a physicochemical barrier in their mid-periphery, just where Fleischer rings occur as the disease progresses.

On the one hand, such a barrier at the base of the cone can be due to idiopathic degenerative and/or dystrophic changes in corneal tissues associated with alkalization and/or oxidative stress. On the other hand, the barrier, regardless of its origin, causes element depletion of the central cornea, impairment of collagen metabolism, and disorganization of extracellular matrix with subsequent keratectasia. These changes in turn *maintain conditions* favorable to the *formation of* the physicochemical barrier, thereby closing a further vicious circle.

Thus, we can conclude that 1) the Fleischer ring appears to be not only a slit-lamp sing of KC, but also its pathogenetic and/or etiological factor, and 2) once started the pathological process in KC is likely to become self-sustaining.

Despite the difficulty of physical research of human corneas in vivo, further studies are needed to reveal the exact cause and effect relationships involved in keratoconus development and progression.

Author contributions:

Study conception and design — S.A., V.M., I.N. Acquisition and handling of data — V.M., I.N., L.P., G . O . Statistical analysis of data — I.N., L.P., N.K. Drafting of manuscript — I.N., L.P., N.K. Critical revision — S.A.

The authors declare no conflict of interest.

REFERENCES

1. Wang MX, Swartz TS. Keratoconus and Keratoectasia: prevention, diagnosis, and treatment. SLACK Incorporated; 2010.
2. Khurana A.K. Theory and practice of optics and refraction. Elsevier, 2008.
3. Edrington T.B., Zadnik K., Barr J.T. Keratoconus. Optom Clin. 1995;4(3):65-73.
4. Barbara A., Rabinowitz Y.S. Textbook on keratoconus: new insights. JP Medical Ltd., 2011.
5. Krachmer J.H., Palay D.A. Cornea atlas. Elsevier Mosby, 2006.
6. Avetisov S.E. Mamikonyan V.R., Novikov I.A. The role of tear acidity and Cu-cofactor of lysyl oxidase activity in the pathogenesis of keratoconus. Vestn. Oftalmol. 2011 Mar-Apr;127(2):3-8.
7. Amsler M. La notion du keratocone. Bull mem soc fr ophthal 1951;64:272-6.
8. Kenney M.C., Nesburn A.B., Burgeson R.E., Butkowski R.J., Ljubimov, A.V. Abnormalities of the extracellular matrix in keratoconus corneas. Cornea. 1997 May;16(3):345-51.
9. Nelidova D., Sherwin T. Keratoconus layer by layer – pathology and matrix metalloproteinases. In: Rumelt S. (Ed). Advances in Ophthalmology. InTech, 2012:105–118.
10. Stachs O., Bochert A., Gerber T., Koczan D., Thiessen H.J., Guthoff R.F. The extracellular matrix structure in keratoconus. Ophthalmologe. 2004 Apr;101(4):384-9.
11. Nath R. Health and disease role of micronutrients and trace elements. APH Publishing Corp., 2000.
12. Berg J.M., Tymoczko J.L., Stryer L. Biochemistry. W.H. Freeman, 2006.
13. Bhagavan N.V. Medical biochemistry. Academic Press, 2001.
14. Litwack G. Human biochemistry and disease. Academic Press, 2008.
15. Talwar G.P., Srivastava L.M. Textbook of biochemistry and human biology. PHI Learning Pvt. Ltd., 2002.
16. Avtar R., Tandon D. Mathematical analysis of corneal oxygenation. Int. J. Health Res. 2008; 1(3):129–138. doi: 10.4314/ijhr.v1i3.55356

17. Brennan N.A. Corneal oxygenation during contact lens wear: comparison of diffusion and EOP-based flux models. Clin. Exp. Optom. 2005 Mar;88(2):103-8.
18. Efron N. Contact lens complications. Butterworth–Heinemann, 2004.
19. Smolin G., Foster C.S., Azar D.T., Dohlman C.H. Smolin and Thoft's the cornea: scientific foundations and clinical practice. Lippincott Williams & Wilkins, 2005.
20. Takatori S.C., de la Jara P.L., Holden B., Ehrmann K., Ho A., Radke C.J. In vivo oxygen uptake into the human cornea. Invest. Ophthalmol. Vis. Sci. 2012 Sep 19;53(10):6331-7
21. Zelko I.N., Mariani T.J., Folz R.J. Superoxide dismutase multigene family: a comparison of the CuZn-SOD (SOD1), Mn-SOD (SOD2), and EC-SOD (SOD3) gene structures, evolution, and expression. Free Radic. Biol. Med. 2002 Aug 1;33(3):337-49.
22. Gass J.D. The iron lines of the superficial cornea. Arch. Ophthalmol. 1964 Mar;71:348-58.
23. Loh A., Hadziahmetovic M., Dunaief J.L. Iron homeostasis and eye disease. Biochim. Biophys. Acta. 2009 Jul;1790(7):637-49.
doi: 0.1016/j.bbagen.2008.11.001
24. Norn, M.S. Hudson–Stahli's line of cornea. I. Incidence and morphology. Acta Ophthalmol (Copenh). 1968;46(1):106-18.
25. Norn M.S. Hudson–Stahli's line of cornea. II. Aetiological studies. Acta Ophthalmol (Copenh). 1968;46(1):119-28.
26. Krachmer J.H., Mannis M.J., Holland E. J. Cornea. Elsevier Mosby, 2005.
27. Kirkwood B.J., Rees I.H. Central corneal iron line arising from hyperopic orthokeratology. Clin. Exp. Optom. 2011 Jul;94(4):376-9.
doi: 10.1111/j.1444-0938.2010.00573.x.
28. Cho P., Cheung S.W., Mountford J., Chui W.S. Incidence of corneal pigmented arc and factors associated with its appearance in orthokeratology. Ophthalmic Physiol. Opt. 2005 Nov;25(6):478-84.
29. Assil K.A., Quantock A.J., Barrett A.M., Schanzlin D.J. Corneal iron lines associated with the intrastromal corneal ring. Am. J. Ophthalmol. 1993 Sep 15;116(3):350-6.
30. Steinberg E.B., Wilson L.A., Waring G.O., Lynn M.J., Coles W.H. Stellate iron lines in the corneal epithelium after radial keratotomy. Am. J. Ophthalmol. 1984 Oct 15;98(4):416-21.
31. Krueger R.R., Tersi I., Seiler T. Corneal iron line associated with steep central islands after photorefractive keratectomy. J. Refract. Surg. 1997 Jul-Aug;13(4):401-3.
32. Probst L.E., Almasswary M.A., Bell J. Pseudo-Fleischer ring after hyperopic laser in situ keratomileusis. J. Cat. Refract. Surg. 1999 Jun;25(6):868-70.
33. Yanoff M., Duker J.S., Augsburger J.J. Ophthalmology. Elsevier Mosby, 2009.
34. Avetisov, E.S., Vinetskaia, M.I., Iomdina, E.N., Makhmudova, F.R., Boltaeva, Z.K., Tarutta, E.P., Copper metabolism in scleral tissue and possibilities of its correction in myopia. Vestn. Oftalmol. 1991 Sep-Oct;107(5):31-4.
35. Lichey H.J., Fischer F., Wiederholt M. Intracellular potentials in the isolated human cornea. Pflugers Arch. 1974;346(4):351-60.